Journal of Experimental Botany, Vol. 60, No. 11, pp. 2987–3004, 2009
doi:10.1093/jxb/erp156 Advance Access publication 22 May, 2009

Journal of Experimental Botany
www.jxb.oxfordjournals.org

REVIEW PAPER

Scientific and technical challenges in remote sensing of plant canopy reflectance and fluorescence

Zbyněk Malenovský[1,2,*,†], Kumud Bandhu Mishra[3,4,*], František Zemek[5], Uwe Rascher[6] and Ladislav Nedbal[3,4]

[1] Remote Sensing Laboratories, Department of Geography, University of Zürich, Winterthurerstrasse 190, 8057 Zürich, Switzerland
[2] Centre for Geo-Information, Wageningen University, Droevendaalsesteeg 3/PO Box 47, 6700 AA Wageningen, The Netherlands
[3] Departments of Plant Physiology and Ecology and Mathematical Biology, Institute of Systems Biology and Ecology ASCR, Zámek 136, 37333 Nové Hrady, Czech Republic
[4] Institute of Physical Biology, University of South Bohemia, Zámek 136, 37333 Nové Hrady, Czech Republic
[5] Laboratory of Plants Ecological Physiology, Institute of Systems Biology and Ecology ASCR, Poříčí 3b, 60300 Brno, Czech Republic
[6] Institute of Chemistry and Dynamics of the Geosphere (ICG-3), Forschungszentrum Jülich GmbH, 52425 Jülich, Germany

Received 14 January 2009; Revised 16 April 2009; Accepted 22 April 2009

Abstract

State-of-the-art optical remote sensing of vegetation canopies is reviewed here to stimulate support from laboratory and field plant research. This overview of recent satellite spectral sensors and the methods used to retrieve remotely quantitative biophysical and biochemical characteristics of vegetation canopies shows that there have been substantial advances in optical remote sensing over the past few decades. Nevertheless, adaptation and transfer of currently available fluorometric methods aboard air- and space-borne platforms can help to eliminate errors and uncertainties in recent remote sensing data interpretation. With this perspective, red and blue-green fluorescence emission as measured in the laboratory and field is reviewed. Remotely sensed plant fluorescence signals have the potential to facilitate a better understanding of vegetation photosynthetic dynamics and primary production on a large scale. The review summarizes several scientific challenges that still need to be resolved to achieve operational fluorescence based remote sensing approaches.

Key words: Chlorophyll fluorescence, optical remote sensing, photosynthesis dynamics, reflectance, vegetation primary production.

Introduction

Monitoring of vegetation on a global scale is essential for understanding dynamic biosphere processes. These are, to a large extent, formed by global photosynthetic energy transformation, which includes carbon dioxide assimilation and oxygen release by vegetation, and plays a role in maintaining the water balance (Bonan, 1995; Liu *et al.*, 1997; Coops and Waring, 2001*a*; Veroustraete *et al.*, 2002; Falloon *et al.*, 2007). Several airborne or space-borne multispectral or hyperspectral sensors are currently able to measure the electromagnetic radiation reflected or emitted from vegetation. The acquired data are used to deduce the large-scale spatio-temporal distribution of vegetation and estimate its biochemical (e.g. content of chlorophyll or water) and biophysical (e.g. leaf area index or foliage

* Both authors contributed equally to this work.
† To whom correspondence should be addressed: E-mail: zbynek.malenovsky@gmail.com
Abbreviations: Chl, chlorophyll; Chl *a*, chlorophyll *a*; ChlF, chlorophyll fluorescence; ChlFs, chlorophyll fluorescence steady-state; DCMU, 3-(3,4-dichlorophenyl)-1,1-dimethylurea; ESA, European Space Agency; *ETR*, electron transport rate; *fAPAR*, fraction of absorbed photosynthetically active radiation; FLD, Fraunhofer line discrimination; *GPP*, gross primary productivity; *IPAR*, incident photosynthetically active radiation; *LAI*, leaf area index; LIDAR, light detection and ranging; *LUE*, light use efficiency; MODTRAN, MODerate spectral resolution atmospheric TRANsmittance; NASA, National Aeronautics and Space Administration; *NDVI*, normalized difference vegetation index; NIR, near infrared; *NPP*, net primary productivity; *NPQ*, non-photochemical quenching; PAM, pulsed amplitude modulation; PPFD, photosynthetically active photon flux density; *PRI*, photochemical reflectance index; PS, photosystem; RT, radiative transfer; SAIL, Scattering by Arbitrary Inclined Leaves; SIF, solar-induced fluorescence; SWIR, shortwave infrared; UV, ultraviolet; VIs, vegetation indices; VIS, visible.
© The Author [2009]. Published by Oxford University Press [on behalf of the Society for Experimental Biology]. All rights reserved.
For Permissions, please e-mail: journals.permissions@oxfordjournals.org

clumping) properties (reviewed in Walter-Shea *et al.*, 1991; Curran *et al.*, 2001). These parameters can serve as indicators of vegetation stress (reviewed in Jago *et al.*, 1999) or as markers of dominant plant species (Martin *et al.*, 1998).

Remotely sensed vegetation properties are essential for ecological modelling of carbon and nutrient cycles, and estimating vegetation production on regional and global scales (Asner, 1998; Lucas and Curran, 1999; Lucas *et al.*, 2000). Several photosynthetic (Xiao *et al.*, 2005), biogeochemical (Ruimy *et al.*, 1996), and production (Potter *et al.*, 1993; Running *et al.*, 2004) models of vegetation have been parameterized by remote-sensing products; however, significant discrepancies were found between model predictions and ground-based measurements (Running *et al.*, 1999; Drolet *et al.*, 2005; Martel *et al.*, 2005; Turner *et al.*, 2006; Friend *et al.*, 2007). Development of more accurate remote sensing methods, supported by laboratory and field measurements of plant reflectance and fluorescence, could minimize these discrepancies (Grace *et al.*, 2007).

Photons of the visible wavelengths (VIS, 0.4–0.7 μm) are strongly absorbed by foliar pigments. This energy is used for photosynthesis, dissipated as heat (mainly under a high photosynthetically active irradiation), or re-emitted as chlorophyll fluorescence (ChlF). ChlF emission represents only 2–3% of leaf electromagnetic reflectance in the red and near infrared spectral regions (Zarco-Tejada *et al.*, 2003). Various laboratory plant-physiological experiments used ChlF measurements as determinants of yields of photosynthetic electron transport and charge separation (Briantais *et al.*, 1986; Schreiber *et al.*, 1986; Krause and Weis, 1991; Govindjee, 1995). Although the intensity of the fluorescence signals is low relative to reflectance, it has been shown convincingly that the vegetation solar-induced fluorescence (SIF) signal can be extracted from aerial or even satellite-based sensor data (Moya *et al.*, 2003; Guanter *et al.*, 2007). This was achieved by using sharply contrasting spectral modulations of both optical signals in and close to the Fraunhofer and oxygen absorption lines of the solar spectrum (Plascyk and Gabriel, 1975; Moya and Cerovic, 2004; Louis *et al.*, 2005). The feasibility of this method has been tested on data obtained from the AIRFLEX fluorometer, an airborne device for fluorescence experimental activities of the European Space Agency (ESA). Nevertheless, several scientific and technical challenges, related to: (i) the correct understanding of the nature of the reflectance and fluorescence of the vegetation, (ii) the operability of the radiative transfer models, (iii) the quality of the optical sensors, and (iv) advanced interpretation of the remotely sensed image data, are addressed by this review paper.

Vegetation-observing spectroradiometers

The era of satellite remote sensing of vegetation began 35 years ago, when the National Aeronautics and Space Administration (NASA) launched the Land Remote Sensing Satellite (LANDSAT)-1 carrying on board a Multi-Spectral Scanner (MSS). Since then, a series of satellite multispectral spectroradiometers with improved spatial and spectral resolution have been launched (Table 1). A new generation of space-borne sensors offers data of several narrow spectral bands within a short re-visit time, which allows for more accurate and temporally frequent vegetation monitoring. For instance, VEGETATION (VGT) on board the Système pour l'Observation de la Terre (SPOT-4) satellite (Qi *et al.*, 1993; Xiao *et al.*, 2002; Boles *et al.*, 2004) provides daily coverage of the globe at 1 km spatial resolution, the Moderate Resolution Imaging Spectroradiometer (MODIS), on board both the Aqua (Earth Observing System PM-1) and Terra (Earth Observing System AM-1) satellites (van Leeuwen *et al.*, 1999; Price, 2003; Zhang *et al.*, 2003), is able to sense the same spot on Earth in one or two days at the highest spatial resolution of 250 m, and the Medium Resolution Imaging Spectrometer (MERIS) operating on the environmental satellite ENVISAT (Dawson, 2000) records the same location every third day in full-resolution of 300 m pixel size. The unique information content for mapping vegetation canopy structure is provided by multi-angular satellite images (Zhang *et al.*, 2002; Lotsch *et al.*, 2003; Nolin, 2004; Diner *et al.*, 2005; Liesenberg *et al.*, 2007). The Multiangle Imaging Spectro-Radiometer (MISR) on board the Terra platform is a system of nine spectrometers viewing the Earth in four spectral bands (blue, green, red, and NIR) simultaneously at nine different angles. The Compact High Resolution Imaging Spectrometer (CHRIS) instrument on board the ESA satellite Project for On-board Autonomy (PROBA; Cutter, 2004; Rautiainen *et al.*, 2008; Verrelst *et al.*, 2008) is the first hyperspectral space-borne sensor providing 17 m spatial resolution data at five multiple viewing angles. An extensive overview of the operational hyperspectral space and airborne imaging spectroradiometers is given in Table 2.

Reflectance-based methods to retrieve vegetation canopy properties

Currently operating air/space-borne optical sensors are recording the reflectance signal resulting from complex photon–vegetation interactions. These reflection, transmission, absorption, and emission processes arise from high canopy spatio-structural heterogeneity (clumping of foliage, leaf angle distribution, spatial distribution of plants, etc.) and also from interactions with surrounding environmental features (litter, bare soil, woody parts, and debris, etc.). Multiple scattering and photon re-absorption causes significant geometric anisotropy in canopy optical signal propagation, which must be taken into account when retrieving the quantitative properties of the vegetation from optical remote-sensing data.

Table 1. Multispectral satellite sensors currently employed in vegetation monitoring

Satellite: Sensor	Band: Spectral bandwidth	Spatial resolution(m)/ Swath width (km)	Temporal sampling/data availability (Information source)
LANDSAT: TM (Thematic Mapper) on Landsat 4 and 5	1: 450–520 nm	30/170–183	16 d/1983–present (http://edc.usgs.gov/products/satellite/tm.php)
	2: 520–600 nm	30/170–183	
	3: 630–690 nm	30/170–183	
	4: 760–900 nm	30/170–183	
	5: 1.55–1.75 μm	30/170–183	
	6: 2.08–2.35 μm	120/170–183	
	7: 10.4–12.5 μm	30/170–183	
LANDSAT: ETM+ (Enhanced Thematic Mapper on Landsat 7)	1: 450–520 nm	30/170–183	16 d/1999–present (http://edc.usgs.gov/products/satellite/landsat7.php)
	2: 520–600 nm	30/170–183	
	3: 630–690 nm	30/170–183	
	4: 769–900 nm	30/170–183	
	5: 1.55–1.75 μm	30/170–183	
	6: 2.08–2.35 μm	60/170–183	
	7: 10.4–12.5 μm	30/170–183	
	8: 520–900 nm	15/170–183	
NOAA: AVHRR (Advanced Very High Resolution Radiometer on NOAA-9-17)	1: 580–680 nm	1100/2700	12 h/1979–present (http://edc.usgs.gov/ products/satellite/avhrr.html)
	2: 725–1100 nm	1100/2700	
	3: 3.55–3.93 μm	1100/2700	
	4: 10.3–11.3 μm	1100/2700	
	5: 11.5–12.5 μm	1100/2700	
TERRA and AQUA: MODIS (Moderate Resolution Imaging Spectrometer)	36 spectral bands in region 405–14038 nm:		1–2 d/1999–present (http://edc.usgs.gov/products/satellite/modis.html)
	Band 1–2	250/2330	
	Band 3–7	500/2330	
	Band 8–36	1000/2330	
TERRA: MISR (Multiangle Imaging Spectro Radiometer)	1: 425.5–467.5 nm	275/360	9 d/1999–present (http://terra.nasa.gov/Brochure/Sect_4-4.html)
	2: 543.2–571.8 nm	275/360	
	3: 660.8–682.7 nm	275/360	
	4: 846.6–886.3 nm	275/360	
ENVISAT: MERIS (Medium-spectral Resolution Imaging Spectrometer)	15 spectral bands in region 390–1040 nm: Bandwidth programmable between 2.5 and 30 nm	300/1150	3 d/2002–present (http://envisat.esa.int/ instruments/meris/)
SPOT: VGT (VEGETATION 1 and 2 on SPOT4 and 5)	1: 430–470 nm	1150/2200	1 d/1998–present (http://smsc.cnes.fr/ VEGETATION/index.htm)
	2: 610–680 nm	1150/2200	
	3: 780–890 nm	1150/2200	
	4: 1.58–1.75 μm	1150/2200	

Empirical retrieval methods

Robust empirical relationships between remotely sensed canopy reflectance and ground-measured biophysical and biochemical parameters of vegetation were established via simple or multiple regression (Jacquemoud *et al.*, 1995*b*), partial least square regression (Huang *et al.*, 2004), or by training an artificial neural network (reviewed in Dorigo *et al.*, 2007). Mathematical functions of two or more spectral bands are used rather than direct reflectance data to minimize the negative impact of interfering factors, such as the surrounding land cover, bare soil, or climatic/atmospheric conditions (Baret and Guyot, 1991; McDonald *et al.*, 1998; Huete *et al.*, 2002). These functions are called vegetation indices (VIs), each designed for optimal correlation with a particular vegetation feature. The capacity of vegetation indices to characterize natural canopies and agricultural crops has been demonstrated in numerous studies aimed at seasonal phenology (Rasmussen, 1998; Carter, 1998; Qi *et al.*, 2000), biomass prediction (Broge and Leblanc, 2001; Haboudane *et al.*, 2004), mapping chlorophyll content (Al-Abbas *et al.*, 1974; Haboudane *et al.*, 2002), as well as stress detection (Eklundh, 1996; McVicar and Jupp, 1998). The simplicity and straightforwardness makes the empirical methods highly efficient; however, they are often limited to a particular site and time for which the relationship was established (Baret and Guyot, 1991).

Physical retrieval methods

Physical methods, which are based on the inverted use of radiative transfer (RT) models, are relevant alternatives to empirical approaches. These models perform a virtual transfer of photons within vegetation, taking into account

Table 2. Actual and future hyperspectral air/space borne sensors involved in vegetation monitoring
More information on hyperspectral sensors can be found on: http://hydrolab.arsusda.gov/rsbasics/sources.php

Satellite sensors	Wavelength range (nm)	Number of bands	Manufactured and/or operated by (Information source)
CHRIS (Compact High Resolution Imaging Spectrometer) on PROBA	415–1050	62	European Space Agency (http://earth.esa.int/missions/thirdpartymission/proba.html)
EnMAP (Environmental Mapping and Analysis Program)	420–1000 900–2450	94 155	German hyperspectral satellite mission (expected operational in 2012)(http://www.enmap.org/)
Hyperion on EO-1 (Earth Observing)	400–2500	220	NASA Goddard Space Flight Center (http://eo1.gsfc.nasa.gov/Technology/Hyperion.html)
Airborne sensors			
AISA (Airborne Imaging Spectrometer for Applications) DUAL (Eagle and Hawk)	400–2450	Up to 500	Spectral Imaging (SPECIM)(http://www.specim.fi/products/aisa-airborne-hyperspectral-systems/aisa-series.html)
AHS 80 (Airborne Hyperspectral Scanner)	441–13170	80	INTA–Instituto Nacional de Tecnica Aeroespacial (http://www.uv.es/leo/sen2flex/ahs.htm)
APEX (Airborne Prism EXperiment)	380–2500	Up to 300	European Space Agency (expected operational in 2009) (http://www.apex-esa.org/)
ARES (Airborne Reflective Emissive Spectrometer)	450–2450 8000–12000	150	DLR – German Airspace Center (expected operational in 2010) (http://www.ares.caf.dlr.de/intro_en.html)
AVIRIS (Airborne Visible Infrared Imaging Spectrometer)	400–2500	Up to 224	NASA Jet Propulsion Lab (http://aviris.jpl.nasa.gov/)
CASI (Compact Airborne Spectrographic Imager) and SASI (SWIR Airborne Spectrographic Imager)	400–1000 and 950–2450	288 and 100	ITRES Research Limited (http://www.itres.com)
DAIS 21115 (Digital Airborne Imaging Spectrometer)	400–12000	211	GER Corp.(http://www.ger.com)
HyMap (Hyperspectral Mapping)	450–2480	120	HyVista Corporation (http://www.hyvista.com/technology/sensors)
PROBE-1	400–2450	128	Earth Search Sciences Inc. (http://www.earthsearch.com/index.php?sp = 10)

canopy biochemical and biophysical characteristics and objects of the surrounding environment. Top-of-the-canopy reflectance can be simulated via coupling a leaf RT model (e.g. PROSPECT; Jacquemoud and Baret, 1990) with a canopy RT model (e.g. DART; Gastellu-Etchegorry *et al.*, 2004). If further coupled with an atmospheric RT model (e.g. MODerate spectral resolution atmospheric TRANsmittance – MODTRAN; Berk *et al.*, 1998), the top-of-the-atmosphere reflectance can be produced as acquired by airborne or satellite sensors. In the inverted mode, the model input parameters are varied to yield the best match between simulated and remotely sensed vegetation reflectance. The best matching solution can be found by an iterative optimization of an RT model (Jacquemoud *et al.*, 1995*a*; Bacour *et al.*, 2002; Fang *et al.*, 2003), using minimization mathematical functions (Weiss *et al.*, 2000; Combal *et al.*, 2002), or the application of a properly trained artificial neural network (Weiss and Baret, 1999; Fang and Liang, 2005). The RT inversions are operationally used in retrieving biophysical features of the vegetated land surfaces from MODIS and MERIS image data (Bacour *et al.*, 2006; Gobron *et al.*, 2008).

Successive steps of RT-based remote sensing retrieval are depicted in the methodological diagram in Fig. 1. Each approach, which includes mathematical expressions of physical laws, is of a universal nature. However, one has to keep in mind that there is frequently a trade-off between model universality and accuracy. Specific assumptions in deriving a physical model can limit its applicability to only certain vegetation canopy types or geometrical arrangements. Moreover, the RT models require a number of inputs, extensive computation, and long development time. An operational compromise may be offered by hybrid approaches, combining the strengths of both empirical and physical retrievals (Houborg *et al.*, 2007).

Quantitative estimations from remotely sensed reflectance data

Vegetation chlorophyll content

Gitelson *et al.* (2003, 2006) suggested the use of empirical vegetation indices, calculated from the reflectance of three wavelengths that were highly correlated with chlorophyll (Chl), carotenoid, and anthocyanin concentrations to estimate the content of foliar pigments in single leaves. The canopy Chl estimation must resolve the phenomenon of canopy reflectance angular anisotropy and sun-sensor-canopy geometry. But, it mainly has to eliminate, or at least minimize, spectral interference from soil, litter, wood, and understorey on the ground (Yoder and Pettigrewcrosby,

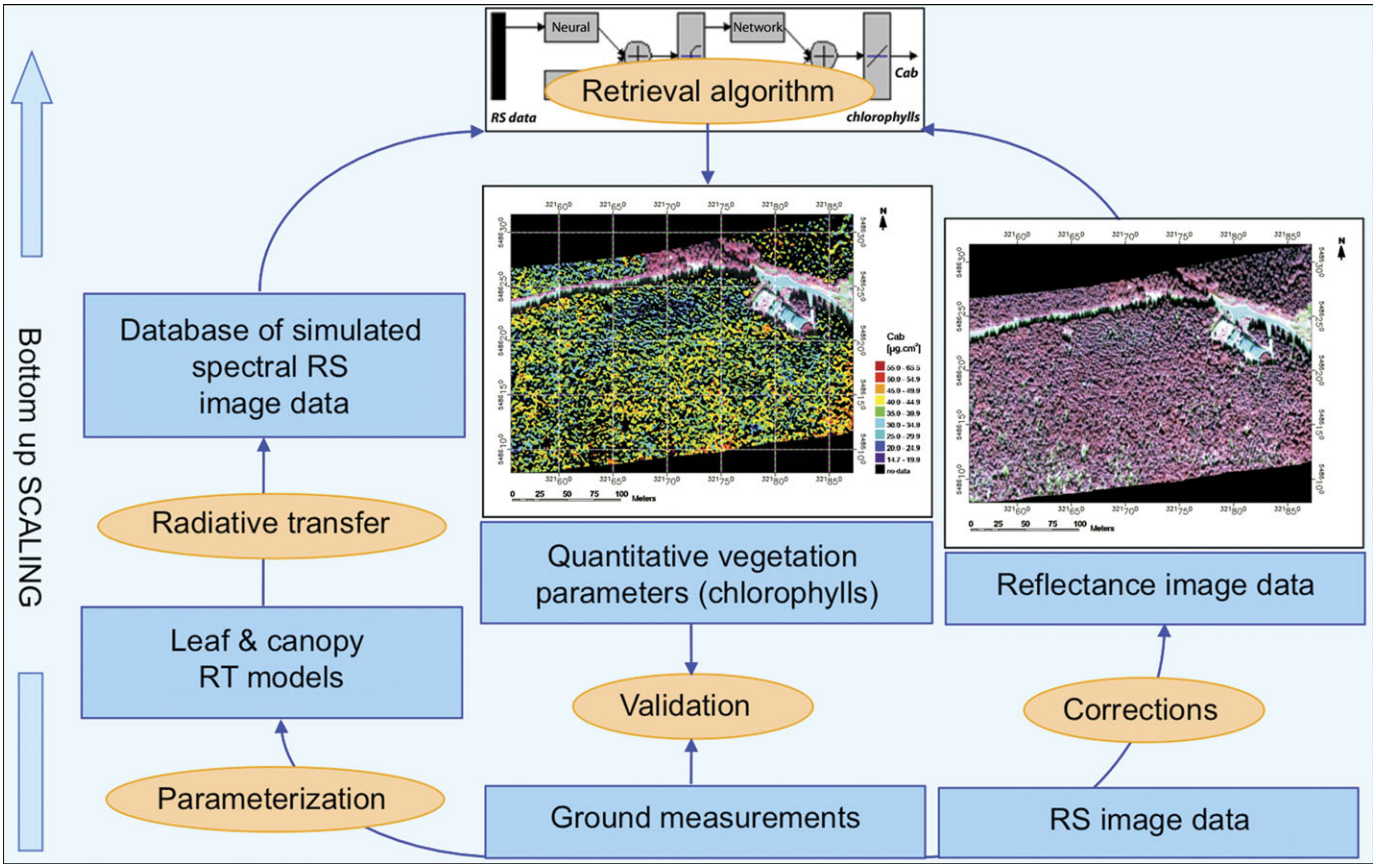

Fig. 1. Bottom-up physical radiative transfer inversion mapping a quantitative characteristic of vegetation canopy from remotely sensed imaging spectroscopy data.

1995; Datt, 1998; Zarco-Tejada *et al.*, 2001; Blackburn, 2002). Several algorithms based on radiative transfer principles were developed to model these cofounding factors and retrieve the vegetation chlorophyll map with use of theses simulations (Curran *et al.*, 1990; Chappelle *et al.*, 1992; Richardson *et al.*, 2002; Sims and Gamon, 2002; Malenovský *et al.*, 2006; see example in Fig. 2). Nevertheless, operational implementation of these physical methods is still technically and computationally demanding.

Fraction of absorbed photosynthetically active radiation

Directly related to the content of foliar pigments is the fraction of absorbed photosynthetically active radiation (*fAPAR*), defined as the ratio between the radiation effectively absorbed by vegetation for photosynthesis and the total incoming photosynthetically active radiation between 400–720 nm (Daughtry *et al.*, 1992; Chen, 1996). Myneni and Williams (1994) linearly related *fAPAR* to the normalized difference vegetation index (NDVI; Rouse *et al.*, 1974; Tucker, 1979; Sellers *et al.*, 1994), computed as the difference between the NIR and red spectral bands divided by the sum of the same bands. The empirical relationship is being used to estimate *fAPAR* from the MODIS reflectance signal attenuated by the presence of clouds or other atmospheric effects. The standard global *fAPAR* MODIS product (spatial resolution of 1 km) is ordinarily derived by inversion of a canopy RT model adjusted for specific biome vegetation types (Knyazikhin *et al.*, 1998; Myneni *et al.*, 2002). Regular *fAPAR* maps for Europe are produced via RT modelling and mathematical optimization from red and NIR SeaWiFS and MERIS satellite images (Gobron *et al.*, 2008) by the Joint Research Centre of the European Commission (available at: http://*fAPAR*.jrc.it). Despite all of these development efforts, validation experiments (Fensholt *et al.*, 2004; Weiss *et al.*, 2007) are still reporting the overestimation of satellite *fAPAR* estimates, caused by residual influence of the atmosphere, sensor viewing angles, and canopy heterogeneity.

Leaf area index

Canopy assimilatory capacity can be approximated by the leaf area index (*LAI*), which is defined as the ratio of half of the total leaf surface in a canopy normalized by the area of canopy projected to the ground surface (Chen and Black, 1992). Although *LAI* does not include estimates of foliage photosynthetic efficiency, it became a key vegetation parameter in modelling biosphere energy, carbon dioxide, and water cycles (Sellers *et al.*, 1994; Bonan, 1995; Band *et al.*, 1991; Liu *et al.*, 1997; Coops and Waring, 2001*b*). Two vegetation indices, NDVI and the Simple Ratio (SR) between NIR and red wavelengths (Baret and Guyot, 1991), were proposed empirically to estimate *LAI* from satellite data on a global scale. Such global estimates are, however, typically reliable

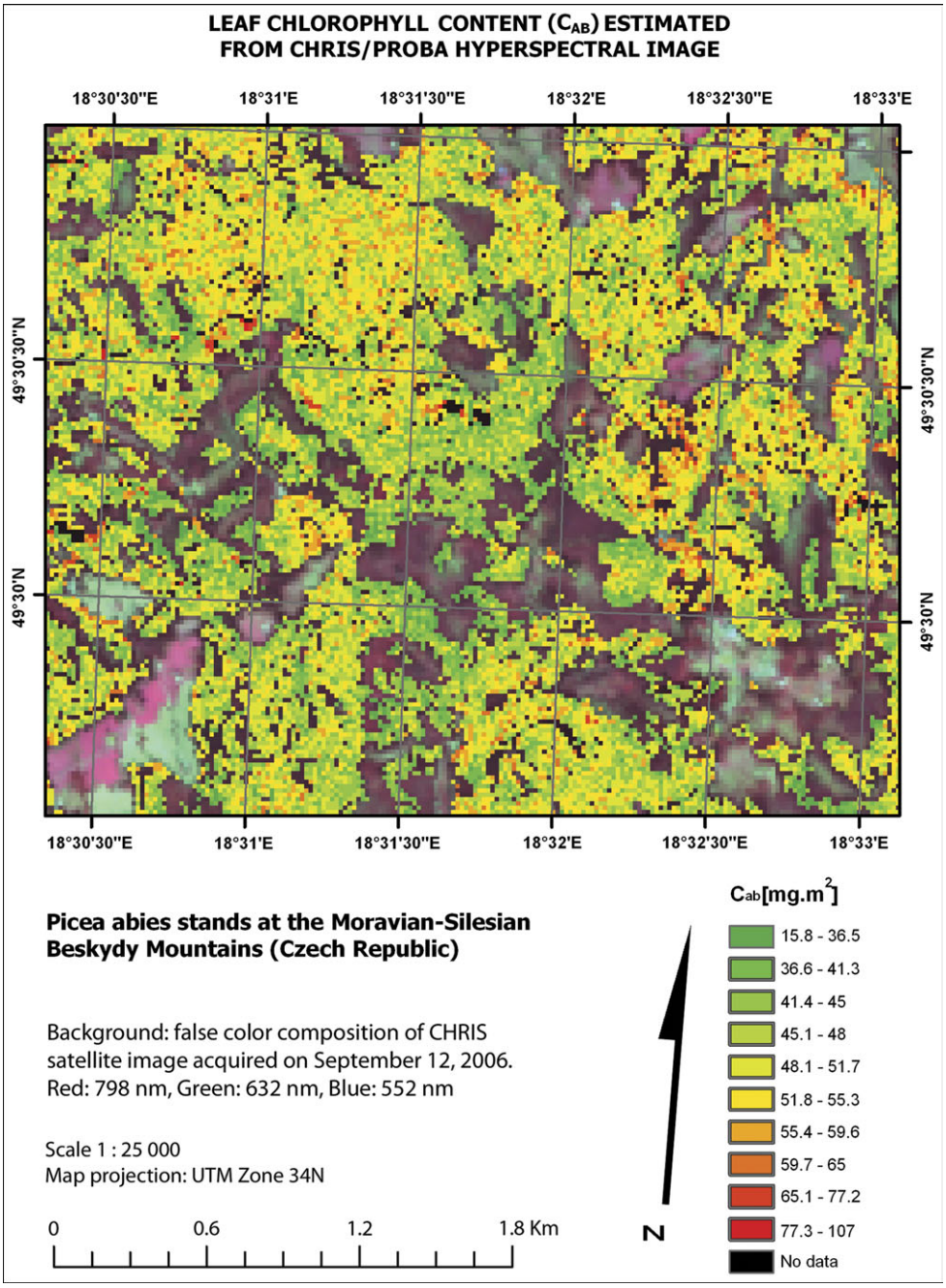

Fig. 2. A subset of the CHRIS/PROBA satellite scene, acquired over the Moravian-Silesian Beskydy Mts. (Czech Republic) on 12 September 2006, illustrating maps of total leaf chlorophyll content of Norway spruce (*Picea abies* L. Karst.) forest stands retrieved by inversion of a leaf/canopy radiative transfer model.

only for low *LAI* values and tend to saturate at dense canopies (reviewed in Wang *et al.*, 2005). Also, in this case, physical RT-based retrieval of *LAI* may offer a more robust solution (Myneni *et al.*, 2002; Bacour *et al.*, 2006), but still represents a challenge for RT modellers.

Plant photosynthetic activity

Plants are dynamically adapting photosynthetic activity according to actual environmental conditions without any significant changes in pigment composition or canopy structure (Rascher *et al.*, 2000; Rascher and Nedbal, 2006; Hilker *et al.*, 2008). Neither Chl content nor *fAPAR* and *LAI* can reflect dynamic changes of photosynthetic activity in the monitored canopy. Gamon *et al.* (1990, 1992) suggested that light use efficiency (*LUE*) of individual leaves, as an indicator of photosynthetic activity, can be empirically correlated with the photochemical reflectance index ($PRI=(R_{531}-R_{570})/(R_{531}+R_{570})$, where R_{531} and R_{570} represent leaf reflectance at the subscripted wavelengths). However, *PRI* values vary

greatly between species with the same photosynthetic capacity (Guo and Trotter, 2004). In addition, Barton and North (2001) proved with RT modelling that *PRI* at canopy level is significantly affected by the geometry of solar illumination, specific leaf angle distribution, and detector viewing angles. As natural canopies are an assembly of differently oriented leaves that additionally change their orientation during development of the plants and as a response to environmental conditions, canopy measurements of *PRI* often failed to quantify photosynthetic efficiency (Methy, 2000) or were greatly affected by seasonal changes in canopy structure (Filella *et al.*, 2004). These results demonstrated the limited capability of reflectance indices and emphasized the need for alternative methods, such as, potentially, the remote sensing of dynamic chlorophyll fluorescence emissions (discussed later).

Modelling vegetation primary production

Regardless of the limitations in detecting photosynthetic activity, massive efforts were undertaken to use information from optical remote sensing for the estimation of vegetation gross primary *productivity* (*GPP*), and, subsequently, net primary *productivity (NPP)* and net ecosystem exchange (*NEE*) of CO_2. Terrestrial biosphere models proved to be highly instrumental in reaching these goals (Gower *et al.*, 1999; Friend *et al.*, 2007). *GPP* was proposed to be a function of *LUE*, *NDVI*, and the incident photosynthetically active radiation (*IPAR*; Goetz *et al.*, 1999; Lopez *et al.*, 2001; Hunt *et al.*, 2002):

$$GPP = LUE \times \sum_{n} (a \times NDVI + b) \times IPAR_{dm}$$

where n is the number of days of the summed satellite observations, and $IPAR_{dm}$ is the daily mean of *IPAR* over the same period. The constants a and b are parameters of a linear model approximating *fAPAR*. Hilker *et al.* (2008) recently hypothesized that inaccurate parameterization of *LUE*, which can be obtained only by indirect means, introduces significant uncertainties in primary production estimates.

On the ground, the production of individual ecosystems is monitored by experimental eddy-covariance tower systems (Baldocchi *et al.*, 2001), organized in large international networks (North America: FLUXNET; Europe: CarboEurope). Running *et al.* (1999) developed a model to retrieve yearly *NPP* using MODIS image data, and explained its relation to the ground-measured *NEE*. Nevertheless, many studies showed significant discrepancies between the modelled satellite-driven estimates and the vegetation production eddy-covariance measurements (Ruimy *et al.*, 1999; Drolet *et al.*, 2005; Martel *et al.*, 2005; Turner *et al.*, 2006; Friend *et al.*, 2007), which suggests that the estimation of vegetation production parameters is still a scientifically challenging issue.

Laboratory-laid foundations of fluorescence techniques

Two major fluorophore groups that dominate the plant fluorescence emissions can potentially be remotely sensed. The first group, which emits photons in the blue and green spectral regions under natural or artificial UV-excitation, is dominated by ferulic acid of the leaf epidermis (Morales *et al.*, 1996). The other short-wavelength candidate fluorophores (phenolics, NADP(H), and perhaps flavonoids) contribute less either because of lower yields, lower concentrations, or because the excitation light does not penetrate to the tissues where they are located (reviewed in Cerovic *et al.*, 1999, 2002; Meyer *et al.*, 2003). Most of the ultraviolet (UV) photons are intercepted in the leaf epidermis, so that photodamage to photosystem (PS) II reaction centres, located deeper in the leaf tissue, is limited (Rundel, 1983). The fluorescence from the epidermis is emitted between 400 nm and 550 nm, with a maximal peak (λ_{max}) between 440–450 nm and a shoulder at around 530 nm (Bongi *et al.*, 1994; Lichtenthaler and Schweiger, 1998; Hideg *et al.*, 2002).

Chlorophyll *a* (Chl *a*) is the second fluorophore contributing largely to plant fluorescence emission. Excitation energy for this fluorescence is delivered from accessory antenna chlorophylls (Chl *a* and Chl *b*), absorbing light of blue and red wavelengths, and from carotenoids, absorbing photons of blue wavelengths. At room temperature, Chl *a* emits fluorescence in the red and NIR (far-red) spectral region between 650–800 nm, in two broad bands with peaks λ_{max}~684–695 nm and λ_{max}~730–740 nm (Lichtenthaler and Rinderle, 1988; Franck *et al.*, 2002). The shorter wavelength emission is attributed to Chl *a* mostly associated to PSII (Dekker *et al.*, 1995), whereas the longer wavelength emission originates from antenna chlorophyll of both PSI and PSII (Pfündel, 1998; Agati *et al.*, 2000; Buschmann, 2007).

Various fluorescence intensity ratios, combining the emissions at blue (F440), green (F520), red (F690), and far-red (F740) wavelengths, were proposed for probing the vegetation vitality status and stress responses (Buschmann *et al.*, 2000; Mishra and Gopal, 2008). For instance, variation in the leaf fluorescence intensity ratio F440/F520 was used to monitor alterations in phenolic secondary metabolites (Stober and Lichtenthaler, 1992; Richards *et al.*, 2003), which occur during plant growth biosynthesis via a shikimate-pathway (Herrmann, 1995). The red ChlF emission between 684-695 nm is strongly re-absorbed by the Chl pigments in the upper layer leaf cells (Agati *et al.*, 1993; Dau, 1994), while the far-red ChlF between 730–740 nm is re-absorbed to a much smaller extent. Consequently, the ratio between the red and far-red ChlF bands (e.g. F690/F740) decreases with increasing leaf Chl content in a curvilinear relationship, which can be used as a good inverse indicator of Chl content changes due to plant growth or stress events (Lichtenthaler and Rinderle, 1988; Buschmann, 2007). Finally, the UV-excited blue-to-red/far-red fluorescence intensity ratios (F440/F690 and F440/F740) were proposed as indicators of the leaf physiological development (Stober *et al.*, 1994; Meyer *et al.*, 2003), but also as marker of the nutrition availability and stress occurrence (Chappelle *et al.*, 1984; Heisel *et al.*, 1996).

Fluorescence measurements in the field

Active excitation of fluorescence transients

In contrast to the static or slowly changing blue–green fluorescence emission, the red and far-red emissions by Chl *a* are highly dynamic, being modulated by photochemical and non-photochemical quenching (see Baker, 2008, for a recent review). These dynamic phenomena yielded important insights into the molecular processes of photosynthesis that occur within time-scales ranging from femtoseconds to minutes depending on the power of an actively applied actinic light (Dau, 1994; Govindjee, 1995; Nedbal and Koblížek, 2006; Rascher and Nedbal, 2006).

Most widely used field observations are active, using devices exciting the photosynthetic machinery with a measuring light and recording the induced fluorescence. Introduction of the pulsed amplitude modulation (PAM) fluorometer allowed non-imaging outdoor measurements in broad daylight (Schreiber *et al.*, 1986). Fluorescence imaging was introduced in the laboratory by Omasa *et al.* (1987) and modified for field surveys in the mid-1990s by Nedbal *et al.* (2000). The laser pulses of actinic light, which can be discriminated from static and panchromatic background light, are applied to elicit fluorescent transients when measuring fluorescence from a distance (Cecchi *et al.*, 1994; Corp *et al.*, 2006). The footprint of such a light detection and ranging (LIDAR) laser beam can be expanded from several centimetres up to metres to cover larger observation areas or to decrease the power of the excitation source (Saito *et al.*, 2005). The first field laser-induced vegetation fluorescence was observed by Measures *et al.* (1973). Ounis *et al.* (2001) developed a dual-excitation fluorescence LIDAR (DE-FLIDAR) measuring Chl *a* fluorescence excited by UV and green wavelength photons of a Nd:YAG laser. Lately, an eye-safe outdoor laser-induced fluorescence transient (LIFT) fluorometer has been constructed. This device is able to measure the fluorescence parameters and non-photochemical quenching (*NPQ*) or electron transport rate (*ETR*) from a distance of about 30–50 m (Ananyev *et al.*, 2005; Kolber *et al.*, 2005) (Fig. 3). A new generation active field fluorescence instrument, developed by Raimondi *et al.* (2007), was successfully employed in summer 2007 during the joint CarboEurope, FLEX, and Sentinel-2 ESA mission campaign CEFLES2 (U Rascher *et al.*, unpublished data). These ground-based active fluorescence-sensing techniques can be used whenever temporal monitoring of fluorescence transients is required regardless of the appearance of cloud cover.

Passive solar-induced fluorescence sensing

In spite of the fact that solar-induced fluorescence (SIF) emission contributes only a small amount to total vegetation reflectance (Buschmann and Lichtenthaler, 1988; Liu *et al.*, 2005), it can be separated from the reflectance signal by accurate measurements inside and near to the solar Fraunhofer and atmospheric absorption lines. These lines are represented by narrow wavelength bands, in which the solar irradiance is attenuated by absorption within the Sun or Earth atmospheres (Plascyk, 1975; Plascyk and Gabriel, 1975). Table 3 shows the major absorption lines of the solar spectrum compared to the spectral range of plant fluorescence emission, indicating their potential applicability for the monitoring of plant fluorescence. Nevertheless, only a few of these lines have so far been explored for feasibility of plant fluorescence detection. According to Moya and Cerovic (2004), blue plant fluorescence could theoretically be monitored within the F line H_β (486.1 nm). The ChlF emissions (F685 and F740) can be measured in O_2-B (687.0 nm) and O_2-A (760.0 nm) atmospheric absorption lines (Moya *et al.*, 2004; Louis *et al.*, 2005), but it is difficult to obtain accurate fluorescence estimates due to the nature of their bandwidth and band-depth. Although an infilling principle of ChlF at the Fraunhofer C line H_α (656.3 nm) called the Fraunhofer line discrimination (FLD), was already developed in the 1970s (Plascyk, 1975; Plascyk and Gabriel, 1975), its application in sensing SIF has been delayed by a lack of suitable field-deployable instrumentation (Carter *et al.*, 1990). The FLD technique was later extended to the estimation of ChlF at the O_2-B (Carter *et al.*, 1996) and O_2-A (Moya *et al.*, 2004) absorption lines. Recently, Alonso *et al.* (2008) improved FLD by introducing correction coefficients to both the reflectance and fluorescence signals. Based on FLD principles, Moya *et al.* (2004) developed a passive multi-wavelength fluorescence detector measuring the infillings of ChlF at both oxygen lines, along with reflectance of PRI bands at 531 nm and 570 nm (Evain *et al.*, 2004; Louis *et al.*, 2005). The sensor requires reflectance measurement of a non-fluorescing target (e.g. bare soil) to quantify correctly the SIF signal of photosynthetically active green plants. On the one hand, the passive fluorometer of Kebabian *et al.* (1999) does not require reference non-vegetative reflectance, but its applicability is limited by a long signal integration time (600 s).

Corp *et al.* (2003) simultaneously used the active and passive approaches to measure fluorescence emissions of several plant species treated and untreated with a nitrogen fertilizer. Results yielded by both methods were consistent. Similarly, Moya *et al.* (2004) found a very high correlation (R >0.99) between the active and passive fluorescence measurements.

Potential use and challenges in remotely sensed fluorescence

Several studies suggested vegetation SIF as an indicator of environmental stress. A significant increase of fluorescence intensity at Fraunhofer line H_α (656.3 nm) was observed with geochemical stress in *Pinus ponderosa* (Watson *et al.*, 1973) and water stress in lemon plants (McFarlane *et al.*, 1980). Carter *et al.* (1996) reported an increase of Chl fluorescence at the O_2-B atmospheric line when palm and grape plants were poisoned by the herbicide 3-(3,4-dichlorophenyl)-1,1-dimethylurea (DCMU). Recently, Meroni and Colombo (2006) were able to discriminate

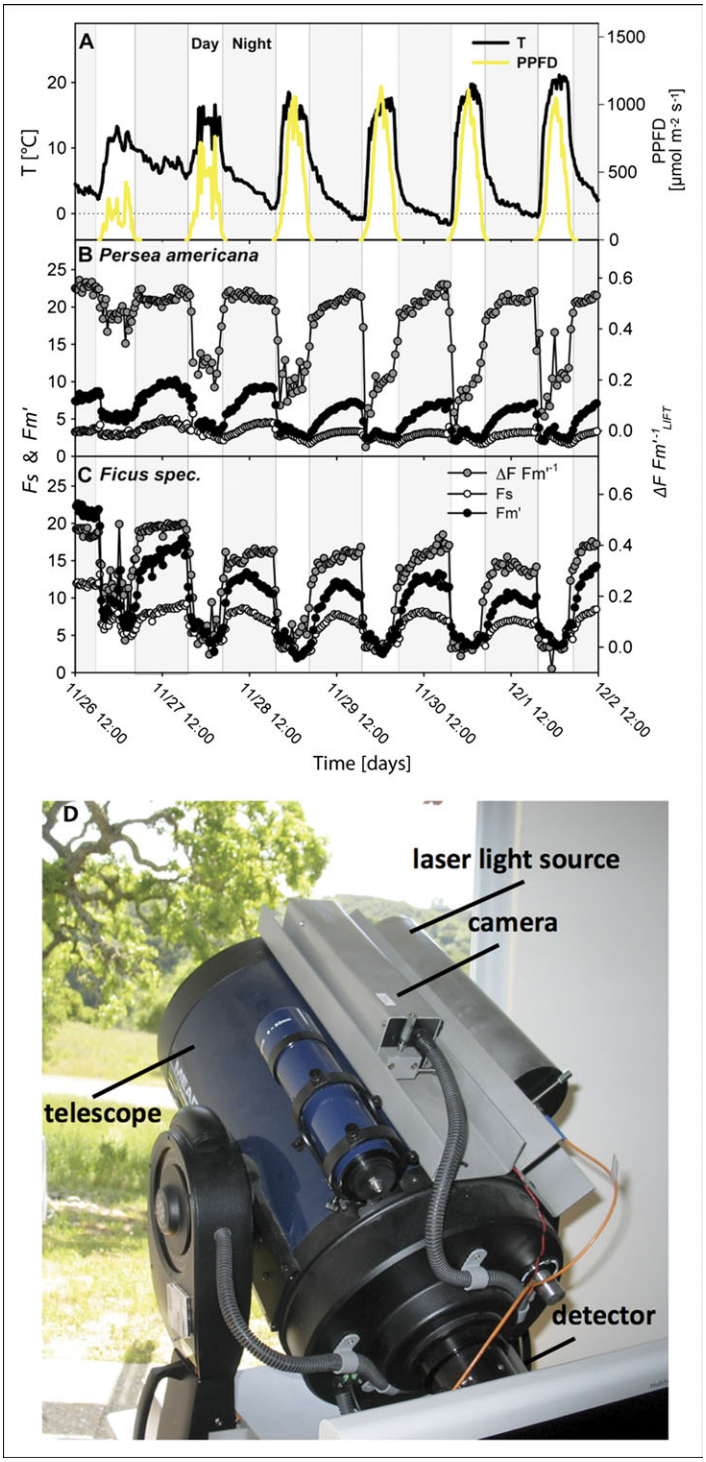

Fig. 3. Temporal influence of changing low/high temperature-irradiation environmental conditions, fluctuating in seven diurnal cycles (A), on two plant species *Persea americana* (B) and *Ficus* sp. (C), expressed by fluorescence parameters measured remotely with the ground-based laser-induced fluorescence transient (LIFT) fluorometer (D). (T, air temperature; PPFD, photosynthetically active photon flux density; *Fs*, LIFT measured steady-state fluorescence; F'_m, LIFT measured maximum fluorescence of light-adapted leaves; $\Delta F=F'^{-1}_m \sim$ actual quantum yield (efficiency), where $\Delta F=F'_m-F\,s$).

between bean leaves, which were either treated or untreated by DCMU, by measuring SIF in the O_2-A and O_2-B lines. Another study conducted in a boreal stand of Scots pine revealed that the relative increase between steady-state fluorescence at the O_2-A and O_2-B lines was proportional to leaf Chl content (Louis *et al.*, 2005). This finding is in accordance with the inverse relationship applied by Lichtenthaler and Rinderle (1988) to derive leaf chlorophyll content from the ChlF intensity ratio F690/F740. If broadly confirmed by additional experiments, this

Table 3. Correspondence between the vegetation blue-green and chlorophyll fluorescence bands that are widely used in plant ecophysiology (Buschmann and Lichtenthaler, 1998; Lichtenthaler *et al.*, 1996) and selected Fraunhofer and oxygen absorption lines with the potential to be used for passive remote-sensing fluorescence measurements (according to Moya and Cerovic, 2004)

Fluorescence common name	Fluorescence band and wavelength range of maxima	Fraunhofer and oxygen absorption lines~central wavelength (FWHM[a]/line label)
Blue-green fluorescence	blue F440 λ_{max}=430–450 nm	H line ~ 396.8 nm (1.440 nm/Ca II), g line ~ 422.7 nm (0.150 nm/Ca I), G' line ~ 434.0 nm (0.350 nm/Hγ), F line ~ 486.1 nm (0.132 nm/Hβ)
	green F520 λ_{max}=520–530 nm	b_1 line ~ 518.4 nm (0.160 nm/MgI)
Chlorophyll fluorescence	red F690 λ_{max}=684–695 nm	C line ~ 656.3 nm (0.144 nm/H_α), iron line ~ 685.5 nm (0.700 nm/FeI)[b], B line ~ 687.0 nm (0.012 nm/O_2-B)
	far-red F740 λ_{max}=730–740 nm	iron line ~ 738.9 nm (0.021 nm/FeI)[b], A line ~ 760.0 nm (1.000 nm/O_2-A)

[a] FWHM: full width at half maximum (line width).
[b] A shallow minor absorption line.

ChlF intensity ratio might potentially be a more accurate substitute for the conventional Chl-sensitive vegetation reflectance indices.

The physiological relationship between solar-induced steady-state ChlF and dynamic photosynthetic processes could potentially be exploited to obtain more accurate estimates of vegetation intercepted photosynthetically active irradiance (i.e. *fAPAR*) (Moya and Cerovic, 2004), or even to approximate vegetation *LUE*. Both parameters, when remotely sensed, may result in local/global maps of vegetation *GPP*, and hence contribute to the spatially explicit monitoring of the CO_2 cycle. Nevertheless, to achieve these future goals one needs to be able to: (i) deconvolute the information contained in the complex steady-state ChlF signal, (ii) simulate the SIF signal scaled from single leaves to the level of heterogeneous canopies, (iii) acquire airborne or satellite fluorescence spectral image data, and (iv) overcome specific technical challenges related to the concept of air-/space-borne remote sensing (i.e. the need for an accurate atmospheric radiative transfer algorithm eliminating co-founding atmospheric influences).

Interpretation of steady-state fluorescence

Steady-state chlorophyll fluorescence (ChlFs) is emitted from a photosynthetically active plant adapted to ambient irradiance when the electron transport processes and the coupled biochemical reactions of the carbon reduction cycle establish a dynamic equilibrium. Various molecular mechanisms of this equilibrium, classified as photochemical and non-photochemical fluorescence quenching (Krause and Weis, 1991; Niyogi, 1999), are driven by both internal (e.g. reaction centre stoichiometry or enzyme activation) and external (e.g. irradiance, temperature, humidity, CO_2 and water availability, nutrients, and various stressors) factors that modulate ChlF intensity. Therefore, ChlF can be considered as a potential indicator of the physiological status of vegetation, measured by remote-sensing techniques over long distances.

Soukupová *et al.* (2008) studied the indicative potential of ChlF by measuring annual ChlF variation of two field-grown evergreen species of the temperate zone: *Picea omorika* and *Rhododendron hybridum*. The amplitudes of the diurnal variation in ChlF were found to be significantly smaller than the seasonal transitional changes. The abrupt temporal behaviour of ChlF corresponded clearly with activation and deactivation of the photosynthetic apparatus of the monitored evergreen plants at the beginning and end of the vegetation season. The seasonal winter–spring ChlF transition appeared when night frosts did not occur for three consecutive days. For healthy and well-irrigated plants, ChlF diurnal variation was reported to track morning and evening irradiance intensities (Cerovic *et al.*, 1996; Flexas *et al.*, 2000; Ounis *et al.*, 2001). However, a pronounced ChlF decrease was observed at midday on sunny days, when irradiance intensity and temperature were high. This noon depression is attributed to complex physiological modulation, combining changes in plant stomatal conductance and CO_2 assimilation together with *NPQ* of chlorophyll fluorescence, which can include photoinhibition (Flexas *et al.*, 2000; Louis *et al.*, 2005). Under drought stress conditions, a negative correlation was revealed between ChlF and increasing irradiance (Flexas *et al.*, 1998, 1999, 2002*a*, *b*; Dobrowski *et al.*, 2005). The stomata that are closed to prevent water loss are limiting the supply of CO_2 for the Calvin–Benson cycle and linear electron transport, which directly affects ChlF (Cornic, 2000). Nevertheless, the effect of drought on ChlF depends on a complex interplay of physiological responses to temperature and incoming irradiance. Hence, in spite of all these achievements, more *in situ* multi-scale field experiments combined with canopy level fluorescence modelling are needed to clarify the true indicative potential of ChlF for remote sensing of plant photosynthesis.

Modelling vegetation fluorescence on a large scale

Physical models of plant fluorescence are able to assist in causal and site non-specific interpretation of the fluorescence signals acquired by remote sensing at the scale of

whole canopies. The models are required to predict the feasibility of airborne and space fluorescence missions and for diagnosis of required sensor technical specifications. Several radiative transfer models have been designed to simulate leaf optical properties, i.e. leaf reflectance and transmittance between 400–2500 nm. They are based on leaf biochemical and structural input parameters (Jacquemoud *et al.*, 2000), but most of them cannot interactively reproduce the ChlF signals (Rosema *et al.*, 1991; Olioso *et al.*, 1992; van der Tol *et al.*, 2009). Pedrós *et al.* (2005) implemented the fluorescence quantum efficiency, the relative contribution of photosystems (stoichiometry of the PSII to PSI reaction centres), leaf temperature, and light levels into the PROSPECT model of Jacquemoud and Baret (1990). This way, they enabled the newly developed FluorMODleaf model to simulate the leaf reflectance and transmittance spectra along with ChlF signals. At the canopy level, fluorescence can be considered as an integral of fluorescence emissions of individual leaves, which are transferred through the canopy. To simulate the fluorescence signal at the top-of-the-canopy level, Verhoef (2004) implemented the FluorMODleaf fluorescence excitation matrix into his Scattering by Arbitrary Inclined Leaves (SAIL) canopy RT model (Verhoef, 1984, 1985). The newly created FluorSAIL model, when coupled with the atmospheric RT model MODTRAN, can provide top-of-the-atmosphere radiance data of 1 nm bandwidth between 400–1000 nm, as potentially sensed by a future space fluorescence mission. The integrated FluorMOD software package was equipped with a graphical user interface (Zarco-Tejada *et al.*, 2006); it has been made available to the public via the Internet (see http://www.ias.csic.es/fluormod/). Still, results of several case studies presented at an ESA fluorescence workshop in Florence (Italy) pointed out that FluorMOD performance can strongly benefit from further improvement. The major drawback was identified as an accurate simulation of the fluorescence spectral profile, which is largely affected by photon re-absorption in leaves and the canopy. Hence, Pedrós *et al.* (2008) attempted to combine the measured and modelled fluorescence emissions with the purpose of obtaining properly shaped leaf chlorophyll SIF signatures, which should, consequently, result in more accurate simulation of the fluorescence signal as being observed by aerial and satellite detectors.

Atmospheric disturbance of remotely sensed fluorescence

Similar to other optical remote-sensing signals, one of the most important negative disturbances of weak fluorescence signals originates in the atmosphere. Inelastic rotational Raman scattering of O_2 and N_2 molecules (Brinkman, 1968), also called the Ring effect (Grainger and Ring, 1962), reduces the depth of Fraunhofer and atmospheric absorption lines affecting infilling extent, particularly at oblique observation angles (Burrows *et al.*, 1996; Sioris and Evans, 2000). Hence, retrieval of SIF in these lines is most effective from nadir images (i.e. downward-facing images viewing Earth surface objects in the direction of the force of gravity), acquired under a clear sky with minimal atmospheric disturbances (Sioris *et al.*, 2003). Even under the most favourable conditions, reflectance and fluorescence canopy signals are always modulated by multiple scattering and refraction on aerosol particles, curvature of the atmosphere, and the air density varying with atmospheric depth (Moya *et al.*, 2004).

The atmospheric corrections of standard remotely sensed spectrometric images can be facilitated by physical radiative transfer models parameterized for atmospheric conditions measured during data acquisition (Myneni *et al.*, 1995; Bacour *et al.*, 2006). Demand for more precise atmospheric corrections increased with the appearance of new imaging spectroradiometers recording signals in many narrow spectral bands (bandwidth of 1–10 nm). Green *et al.* (1998) demonstrated a procedure of atmospheric calibration and sensitivity analysis for the Airborne Visible Infrared Imaging Spectrometer (AVIRIS). The atmospheric corrections for satellite sensors operating outside the Earth's atmosphere rely largely on the MODTRAN RT model. Guanter *et al.* (2007) coupled the MODTRAN code with FLD in the O_2-A absorption line to retrieve ChlF intensity from a satellite MERIS Full Resolution image and airborne CASI-1500 images of agro-ecosystems (Barrax test site, Spain). Although a close linear regression (R^2=0.854) was found between ChlF values resulting from both data sources, it was concluded that further improvement of the atmospheric radiative transfer is needed to make quantitative vegetation fluorescence retrieval from space fully operational (L Guanter, personal communication).

Outlook of an experimental space fluorescence sensor

A scientific team from the Laboratoire de Météorologie Dynamique in Paris developed a passive airborne SIF recording instrument called AIRFLEX that was successfully tested for the first time during the SEN2FLEX campaign and then employed in combination with extensive ground and airborne supportive measurements during the CEFLES2 campaign (U Rascher *et al.*, unpublished results). The sensor outputs proved that vegetation fluorescence could be measured from a flying platform in both oxygen absorption lines. AIRFLEX represents the aerial predecessor of the Fluorescence Explorer (FLEX) satellite, proposed originally to ESA as one of the 7th Earth Explorer candidate missions (Rascher *et al.*, 2008). The FLEX imaging fluorometer was expected to acquire narrow SIF bands (bandwidth of 0.13 nm) located in individual Fraunhofer and atmospheric absorption lines between 480–760 nm. It was originally proposed to accompany this passive fluorescence system with a multi-angle imaging spectrometer (spectral range of 400–2400 nm) and a thermal infrared imaging system (three thermal bands between 8.8–12.0 μm) as supportive systems facilitating fluorescence signal interpretation. Although the FLEX concept was not approved as a future ESA Earth Explorer mission, its

continuation is anticipated as a scientific technological experiment within the ESA Technology Research Programme.

Concluding remarks

The success of any future space fluorometer operating at Earth orbit depends on the existence of reliable, but operational, data-processing algorithms able to map the actual state of vegetation photosynthesis. The plant research community addressed by this review is expected to play an important role in:

(i) extending our understanding of the steady-state solar-induced fluorescence signal under natural conditions, which is required for unambiguous interpretation of remotely sensed data;

(ii) developing physical models able to simulate fluorescence emission signals scaled up from single leaves to heterogeneous canopies;

(iii) developing advanced air- and space-borne fluorescence detectors achieving a high signal-to-noise ratio in relevant spectral bands;

(iv) and advancing fluorescence image processing algorithms capable of identifying optimal proxies for vegetation parameters of interest.

Acknowledgements

The following project resources supported this work: AVOZ-60870520 (Academy of Sciences of the Czech Republic), GOCE-036866 (6FP EC project ECOCHANGE), QH92034 (MZeCR), MSM-6007665808, 2B06068, OC08055, and OC09001 projects. The authors are thankful to Dr Ronald Pieruschka (Forschungszentrum Jülich GmbH, Germany) for providing information for Fig. 3, Dr Julie Olejníčková (Institute of Systems Biology and Ecology, Czech Republic) for consultation on steady-state fluorescence interpretations, and Dr Zoran G Cerovic (Université Paris-Sud 11, France) for his critical reading of the review manuscript. The FLEX specifications communicated with the co-ordinator of the mission preparatory activities, Professor José Moreno (University of Valencia, Spain), are also acknowledged.

References

Agati G, Cerovic ZG, Moya I. 2000. The effect of decreasing temperature up to chilling values on the *in vivo* F685/F735 chlorophyll fluorescence ratio in *Phaseolus vulgaris* and *Pisum sativum*: The role of the photosystem I contribution to the 735 nm fluorescence band. *Photochemistry and Photobiology* **72,** 75–84.

Agati G, Fusi F, Mazzinghi P, Dipaolo ML. 1993. A simple approach to the evaluation of the reabsorption of chlorophyll fluorescence-spectra in intact leaves. *Journal of Photochemistry and Photobiology B-Biology* **17,** 163–171.

Al-Abbas AH, Barr R, Hall JD, Crane FL, Baumgard MF. 1974. Spectra of normal and nutrient-deficient maize leaves. *Agronomy Journal* **66,** 16–20.

Alonso L, Gómez-Chova L, Vila-Frances JL, Amorós-Lopez J, Guanter L, Calpe J, Moreno J. 2008. Improved Fraunhofer line discrimination method for vegetation fluorescence quantification. *IEEE Geoscience and Remote Sensing Letters* **5,** 4.

Ananyev G, Kolber ZS, Klimov D, Falkowski PG, Berry JA, Rascher U, Martin R, Osmond B. 2005. Remote sensing of heterogeneity in photosynthetic efficiency, electron transport and dissipation of excess light in *Populus deltoides* stands under ambient and elevated CO_2 concentrations, and in a tropical forest canopy, using a new laser-induced fluorescence transient device. *Global Change Biology* **11,** 1195–1206.

Asner GP. 1998. Biophysical and biochemical sources of variability in canopy reflectance. *Remote Sensing of Environment* **64,** 234–253.

Bacour C, Jacquemoud S, Tourbier Y, Dechambre M, Frangi JP. 2002. Design and analysis of numerical experiments to compare four canopy reflectance models. *Remote Sensing of Environment* **79,** 72–83.

Bacour C, Baret F, Beal D, Weiss M, Pavageau K. 2006. Neural network estimation of LAI, *fAPAR*, fCover and LAIxC(ab), from top of canopy MERIS reflectance data: principles and validation. *Remote Sensing of Environment* **105,** 313–325.

Baker NR. 2008. Chlorophyll fluorescence: a probe of photosynthesis *in vivo*. *Annual Review of Plant Biology* **59,** 89–113.

Baldocchi D, Falge E, Gu LH, *et al*. 2001. FLUXNET: a new tool to study the temporal and spatial variability of ecosystem-scale carbon dioxide, water vapour, and energy flux densities. *Bulletin of the American Meteorological Society* **82,** 2415–2434.

Band LE, Peterson DL, Running SW, Coughlan J, Lammers R, Dungan J, Nemani R. 1991. Forest ecosystem processes at the watershed scale: basis for distributed simulation. *Ecological Modelling* **56,** 171–196.

Baret F, Guyot G. 1991. Potentials and limits of vegetation indexes for LAI and APAR assessment. *Remote Sensing of Environment* **35,** 161–173.

Barton CVM, North PRJ. 2001. Remote sensing of canopy light use efficiency using the photochemical reflectance index: model and sensitivity analysis. *Remote Sensing of Environment* **78,** 264–273.

Berk A, Bernstein LS, Anderson GP, Acharya PK, Robertson DC, Chetwynd JH, Adler-Golden SM. 1998. MODTRAN cloud and multiple scattering upgrades with application to AVIRIS. *Remote Sensing of Environment* **65,** 367–375.

Blackburn GA. 2002. Remote sensing of forest pigments using airborne imaging spectrometer and LIDAR imagery. *Remote Sensing of Environment* **82,** 311–321.

Boles SH, Xiao X, Liu J, Zhang Q, Munkhtuya S, Chen S, Ojima D. 2004. Land cover characterization of temperate east Asia using multi-temporal VEGETATION sensor data. *Remote Sensing of Environment* **90,** 477–489.

Bonan GB. 1995. Land atmosphere interactions for climate system models: coupling biophysical, biogeochemical, and ecosystem dynamical processes. *Remote Sensing of Environment* **51,** 57–73.

Bongi G, Palliotti A, Rocchi P, Moya I, Goulas Y. 1994. Spectral characteristics and a possible topological assignment of blue-green fluorescence excited by UV laser on leaves of unrelated species. *Remote Sensing of Environment* **47,** 55–64.

Briantais M, Vernotte C, Krause H, Weis E. 1986. Chlorophyll *a* fluorescence of higher plants: chloroplasts and leaves. In: Govindjee, Amesz J, Fork DC, eds. *Light emission by plants and bacteria*. New York: Academic Press, 539–583.

Brinkman RT. 1968. Rotational Raman scattering in planetary atmospheres. *Astrophysical Journal* **154,** 1087–1093.

Broge NH, Leblanc E. 2001. Comparing prediction power and stability of broadband and hyperspectral vegetation indices for estimation of green leaf area index and canopy chlorophyll density. *Remote Sensing of Environment* **76,** 156–172.

Burrows J, Vountas M, Haug H, Chance K, Marquard L, Muirhead K, Platt U, Richter A, Rozanov V. 1996. *Study of the Ring effect*. Technical Report ESA contract 10996/94/NL/CN, Eurorean Space Agency, Noordwijk, Netherlands.

Buschmann C. 2007. Variability and application of the chlorophyll fluorescence emission ratio red/far-red of leaves. *Photosynthesis Research* **92,** 261–271.

Buschmann C, Langsdorf G, Lichtenthaler HK. 2000. Imaging of the blue, green, and red fluorescence emission of plants: an overview. *Photosynthetica* **38,** 483–491.

Buschmann C, Lichtenthaler HK. 1988. Reflectance and chlorophyll fluorescence signatures in leaves. In: Lichtenthaler HK, ed. *Applications of chlorophyll fluorescence*. Dordrecht: Kluwer Academic Publishing, 325–332.

Carter GA. 1998. Reflectance wavebands and indices for remote estimation of photosynthesis and stomatal conductance in pine canopies. *Remote Sensing of Environment* **63,** 61–72.

Carter GA, Jones JH, Mitchell RJ, Brewer CH. 1996. Detection of solar-excited chlorophyll *a* fluorescence and leaf photosynthetic capacity using a Fraunhofer line radiometer. *Remote Sensing of Environment* **55,** 89–92.

Carter GA, Theisen AF, Mitchell RJ. 1990. Chlorophyll fluorescence measured using the Fraunhofer line-depth principle and relationship to photosynthetic rate in the field. *Plant, Cell and Environment* **13,** 79–83.

Cecchi G, Mazzinghi P, Pantani L, Valentini R, Tirelli D, Deangelis P. 1994. Remote-sensing of chlorophyll *a* fluorescence of vegetation canopies. 1. Near and far-field measurement techniques. *Remote Sensing of Environment* **47,** 18–28.

Cerovic ZG, Goulas Y, Gorbunov M, Briantais J-M, Camenen L, Moya I. 1996. Fluorosensing of water stress in plants. Diurnal changes of the mean lifetime and yield of chlorophyll fluorescence, measured simultaneously and at distance with a t-LIDAR and a modified PAM-fluorimeter, in maize, sugar beet and *Kalanchoë*. *Remote Sensing of Environment* **58,** 311–321.

Cerovic ZG, Samson G, Morales F, Tremblay N, Moya I. 1999. Ultraviolet-induced fluorescence for plant monitoring: present state and prospects. *Agronomie* **19,** 543–578.

Cerovic ZG, Ounis A, Cartelat A, Latouche G, Goulas Y, Meyer S, Moya I. 2002. The use of chlorophyll fluorescence excitation spectra for the non-destructive *in situ* assessment of UV-absorbing compounds in leaves. *Plant, Cell and Environment* **25,** 1663–1676.

Chappelle EW, Kim MS, McMurtrey JE. 1992. Ratio analysis of reflectance spectra (RARS): an algorithm for the remote estimation of the concentrations of chlorophyll *a*, chlorophyll *b*, and carotenoids in soybean leaves. *Remote Sensing of Environment* **39,** 239–247.

Chappelle EW, McMurtrey JE, Wood FM, Newcomb WW. 1984. Laser-induced fluorescence of green plants. 2. Lif caused by nutrient deficiencies in corn. *Applied Optics* **23,** 139–142.

Chen JM. 1996. Canopy architecture and remote sensing of the fraction of photosynthetically active radiation absorbed by boreal conifer forests. *IEEE Transactions on Geoscience and Remote Sensing* **34,** 1353–1368.

Chen JM, Black TA. 1992. Foliage area and architecture of plant canopies from sunfleck size distributions. *Agricultural and Forest Meteorology* **60,** 249–266.

Combal B, Baret F, Weiss M. 2002. Improving canopy variables estimation from remote sensing data by exploiting ancillary information. Case study on sugar beet canopies. *Agronomie* **22,** 205–215.

Coops NC, Waring RH. 2001*a*. Estimating forest productivity in the eastern Siskiyou Mountains of southwestern Oregon using a satellite driven process model, 3-PGS. *Canadian Journal of Forest Research* **31,** 143–154.

Coops NC, Waring RH. 2001*b*. The use of multiscale remote sensing imagery to derive regional estimates of forest growth capacity using 3-PGS. *Remote Sensing of Environment* **75,** 324–334.

Cornic G. 2000. Drought stress inhibits photosynthesis by decreasing stomatal aperture: not by affecting ATP synthesis. *Trends in Plant Science* **5,** 187–188.

Corp LA, McMurtrey JE, Middleton EM, Mulchi CL, Chappelle EW, Daughtry CST. 2003. Fluorescence sensing systems: *in vivo* detection of biophysical variations in field corn due to nitrogen supply. *Remote Sensing of Environment* **86,** 470–479.

Corp LA, Middleton EM, McMurtrey JE, Campbell PKE, Butcher LM. 2006. Fluorescence sensing techniques for vegetation assessment. *Applied Optics* **45,** 1023–1033.

Curran PJ, Dungan JL, Gholz HL. 1990. Exploring the relationship between reflectance red edge and chlorophyll content in Slash Pine. *Tree Physiology* **7,** 33–48.

Curran PJ, Dungan JL, Peterson DL. 2001. Estimating the foliar biochemical concentration of leaves with reflectance spectrometry: testing the Kokaly and Clark methodologies. *Remote Sensing of Environment* **76,** 349–359.

Cutter M. 2004. A low cost hyperspectral mission. *Acta Astronautica* **55,** 631–636.

Datt B. 1998. Remote sensing of chlorophyll *a*, chlorophyll *b*, chlorophyll (*a* + *b*), and total carotenoid content in eucalyptus leaves. *Remote Sensing of Environment* **66,** 111–121.

Dau H. 1994. Short-term adaptation of plants to changing light intensities and its relation to photosystem II photochemistry and

fluorescence emission. *Journal of Photochemistry and Photobiology B-Biology* **26,** 3–27.

Daughtry CST, Gallo KP, Goward SN, Prince SD, Kustas WP. 1992. Spectral estimates of absorbed radiation and phytomass production in corn and soybean canopies. *Remote Sensing of Environment* **39,** 141–152.

Dawson TP. 2000. The potential for estimating chlorophyll content from a vegetation canopy using the Medium Resolution Imaging Spectrometer (MERIS). *International Journal of Remote Sensing* **21,** 2043–2051.

Dekker JP, Hassoldt A, Pettersson A, van Roon H, Groot M-L, van Grondelle R. 1995. On the nature of the F695 and F685 emission of Photosystem II. In: Mathis P, ed. *Photosynthesis: from light to biosphere*. Dordrecht, The Netherlands: Kluwer Academic Publishers, 53–56.

Diner DJ, Braswell BH, Davies R, *et al*. 2005. The value of multiangle measurements for retrieving structurally and radiatively consistent properties of clouds, aerosols, and surfaces. *Remote Sensing of Environment* **97,** 495–518.

Dobrowski SZ, Pushnik JC, Zarco-Tejada PJ, Ustin SL. 2005. Simple reflectance indices track heat and water stress-induced changes in steady-state chlorophyll fluorescence at the canopy scale. *Remote Sensing of Environment* **97,** 403–414.

Dorigo WA, Zurita-Milla R, de Wit AJW, Brazile J, Singh R, Schaepman ME. 2007. A review on reflective remote sensing and data assimilation techniques for enhanced agroecosystem modeling. *International Journal of Applied Earth Observation and Geoinformation* **9,** 165–193.

Drolet GG, Huemmrich KF, Hall FG, Middleton EM, Black TA, Barr AG, Margolis HA. 2005. A MODIS-derived photochemical reflectance index to detect inter-annual variations in the photosynthetic light-use efficiency of a boreal deciduous forest. *Remote Sensing of Environment* **98,** 212–224.

Eklundh L. 1996. *AVHRR NDVI for monitoring and mapping of vegetation and drought in East African environments*. PhD thesis, University of Lund, Sweden, 187.

Evain S, Flexas J, Moya I. 2004. A new instrument for passive remote sensing. 2. Measurement of leaf and canopy reflectance changes at 531 nm and their relationship with photosynthesis and chlorophyll fluorescence. *Remote Sensing of Environment* **91,** 175–185.

Falloon P, Jones CD, Cerri CE, *et al*. 2007. Climate change and its impact on soil and vegetation carbon storage in Kenya, Jordan, India and Brazil. *Agriculture*. *Ecosystems and Environment* **122,** 114–124.

Fang H, Liang S. 2005. A hybrid inversion method for mapping leaf area index from MODIS data: experiments and application to broadleaf and needle leaf canopies. *Remote Sensing of Environment* **94,** 405–424.

Fang H, Liang S, Kuusk A. 2003. Retrieving leaf area index using a genetic algorithm with a canopy radiative transfer model. *Remote Sensing of Environment* **85,** 257–270.

Fensholt R, Sandholt I, Rasmussen MS. 2004. Evaluation of MODIS LAI, *fAPAR* and the relation between *fAPAR* and NDVI in a semi-arid environment using *in situ* measurements. *Remote Sensing of Environment* **91,** 490–507.

Filella I, Peñuelas J, Lorens L, Estiarte M. 2004. Reflectance assessment of seasonal and annual changes in biomass and CO_2 uptake of a Mediterranean shrubland submitted to experimental warming and drought. *Remote Sensing of Environment* **90,** 308–318.

Flexas J, Bota J, Escalona JM, Sampol B, Medrano H. 2002*b*. Effects of drought on photosynthesis in grapevines under field conditions: an evaluation of stomatal and mesophyll limitations. *Functional Plant Biology* **29,** 461–471.

Flexas J, Briantais JM, Cerovic ZG, Medrano H, Moya I. 2000. Steady-state and maximum chlorophyll fluorescence responses to water stress in grapevine leaves: a new remote sensing system. *Remote Sensing of Environment* **73,** 283–297.

Flexas J, Escalona JM, Evain S, Gulias J, Moya I, Osmond CB, Medrano H. 2002*a*. Steady-state chlorophyll fluorescence (*Fs*) measurements as a tool to follow variations of net CO_2 assimilation and stomatal conductance during water-stress in C_3 plants. *Physiologia Plantarum* **114,** 231–240.

Flexas J, Escalona JM, Medrano H. 1998. Down-regulation of photosynthesis by drought under field conditions in grapevine leaves. *Australian Journal of Plant Physiology* **25,** 893–900.

Flexas J, Escalona JM, Medrano H. 1999. Water stress induces different levels of photosynthesis and electron transport rate regulations in grapevines. *Plant, Cell and Environment* **22,** 39–48.

Franck F, Juneau P, Popovic R. 2002. Resolution of the Photosystem I and Photosystem II contributions to chlorophyll fluorescence of intact leaves at room temperature. *Biochimica et Biophysica Acta* **1556,** 239–246.

Friend AD, Arneth A, Kiang NY, *et al*. 2007. FLUXNET and modelling the global carbon cycle. *Global Change Biology* **13,** 610–633.

Gamon JA, Field CB, Bilger W, Björkman O, Fredeen A, Penäuelas J. 1990. Remote sensing of the xanthophyll cycle and chlorophyll fluorescence in sunflower leaves and canopies. *Oecologia* **85,** 1–7.

Gamon JA, Penäuelas J, Field CB. 1992. A narrow-waveband spectral index that tracks diurnal changes in photosynthetic efficiency. *Remote Sensing of Environment* **41,** 35–44.

Gastellu-Etchegorry JP, Martin E, Gascon F. 2004. DART: a 3D model for simulating satellite images and studying surface radiation budget. *International Journal of Remote Sensing* **25,** 73–96.

Gitelson AA, Gritz Y, Merzlyak MN. 2003. Relationships between leaf chlorophyll content and spectral reflectance and algorithms for non-destructive chlorophyll assessment in higher plant leaves. *Journal of Plant Physiology* **160,** 271–282.

Gitelson AA, Keydan GP, Merzlyak MN. 2006. Three-band model for noninvasive estimation of chlorophyll, carotenoids, and anthocyanin contents in higher plant leaves. *Geophysical Research Letters* **33,** L11402.

Gobron N, Pinty B, Aussedat O, Taberner M, Faber O, Mélin F, Lavergne T, Robustelli M, Snoeij P. 2008. Uncertainty estimates for the FAPAR operational products derived from MERIS: impact of top-of-atmosphere radiance uncertainties and validation with field data. *Remote Sensing of Environment* **112,** 1871–1883.

Goetz SJ, Prince SD, Goward SN, Thawley MM, Small J. 1999. Satellite remote sensing of primary production: an improved production efficiency modeling approach. *Ecological Modeling* **122,** 239–255.

Govindjee. 1995. 63 years since Kautsky: chlorophyll *a* fluorescence. *Australian Journal of Plant Physiology* **22,** 711–711.

Gower ST, Kucharik CJ, Norman JM. 1999. Direct and indirect estimation of leaf area index, *fAPAR*, and net primary production of terrestrial ecosystems. *Remote Sensing of Environment* **70,** 29–51.

Grace J, Nichol C, Disney M, Lewis P, Quaife T, Bowyer P. 2007. Can we measure terrestrial photosynthesis from space directly, using spectral reflectance and fluorescence? *Global Change Biology* **13,** 1484–1497.

Grainger JF, Ring J. 1962. Anomalous Fraunhofer line profiles. *Nature* **193,** 762.

Green RO, Eastwood ML, Sarture CM, *et al*. 1998. Imaging Spectroscopy and the Airborne Visible/Infrared Imaging Spectrometer (AVIRIS). *Remote Sensing of Environment* **65,** 227–248.

Guanter L, Alonso L, Gomez-Chova L, Amoros-Lopez J, Vila J, Moreno J. 2007. Estimation of solar-induced vegetation fluorescence from space measurements. *Geophysical Research Letters* **34,** L08401.

Guo JM, Trotter CM. 2004. Estimating photosynthetic light-use efficiency using the photochemical reflectance index: variations among species. *Functional Plant Biology* **31,** 255–265.

Haboudane D, Miller JR, Pattey E, Zarco-Tejada PJ, Strachan IB. 2004. Hyperspectral vegetation indices and novel algorithms for predicting green LAI of crop canopies: modeling and validation in the context of precision agriculture. *Remote Sensing of Environment* **90,** 337–352.

Haboudane D, Miller JR, Tremblay N, Zarco-Tejada PJ, Dextraze L. 2002. Integrated narrow-band vegetation indices for prediction of crop chlorophyll content for application to precision agriculture. *Remote Sensing of Environment* **81,** 416–426.

Heisel F, Sowinska M, Miehe JA, Lang M, Lichtenthaler HK. 1996. Detection of nutrient deficiencies of maize by laser induced fluorescence imaging. *Journal of Plant Physiology* **148,** 622–631.

Herrmann KM. 1995. The Shikimate pathway: early steps in the biosynthesis of aromatic-compounds. *The Plant Cell* **7,** 907–919.

Hideg E, Juhasz M, Bornman JF, Asada K. 2002. The distribution and possible origin of blue-green fluorescence in control and stressed barley leaves. *Photochemical and Photobiological Sciences* **1,** 934–941.

Hilker T, Coops NC, Wulder MA, Black AT, Guy RD. 2008. The use of remote sensing in light use efficiency based models of gross primary production: a review of current status and future requirements. *Science of the Total Environment* **404,** 411–423.

Houborg R, Soegaard H, Boegh E. 2007. Combining vegetation index and model inversion methods for the extraction of key vegetation biophysical parameters using Terra and Aqua MODIS reflectance data. *Remote Sensing of Environment* **106,** 39–58.

Huang Z, Turner BJ, Dury SJ, Wallis IR, Foley WJ. 2004. Estimating foliage nitrogen concentration from HYMAP data using continuum removal analysis. *Remote Sensing of Environment* **93,** 18–29.

Huete A, Didan K, Miura T, Rodriguez EP, Gao X, Ferreira LG. 2002. Overview of the radiometric and biophysical performance of the MODIS vegetation indices. *Remote Sensing of Environment* **83,** 195–213.

Hunt ER, Fahnestock JT, Kelly RD, Welker JM, Reiners WA, Smith WK. 2002. Carbon sequestration from remotely sensed NDVI and net ecosystem exchange. In: Muttiah RS, ed. *From laboratory, spectroscopy to remotely sensed spectra of terrestrial ecosystems*. Dordrecht, Netherland: Kluwer Academic Publishers, 161–174.

Jacquemoud S, Bacour C, Poilvé H, Frangi J-P. 2000. Comparison of four radiative transfer models to simulate plant canopies reflectance: direct and inverse mode. *Remote Sensing of Environment* **65,** 280–291.

Jacquemoud S, Baret F. 1990. PROSPECT: a model of leaf optical-properties spectra. *Remote Sensing of Environment* **34,** 75–91.

Jacquemoud S, Baret F, Andrieu B, Danson FM, Jaggard K. 1995*a*. Extraction of vegetation biophysical parameters by inversion of the PROSPECT + SAIL models on sugar beet canopy reflectance data. Application to TM and AVIRIS sensors. *Remote Sensing of Environment* **52,** 163–172.

Jacquemoud S, Verdebout J, Schmuck G, Andreoli G, Hosgood B. 1995*b*. Investigation of leaf biochemistry by statistics. *Remote Sensing of Environment* **54,** 180–188.

Jago RA, Cutler MEJ, Curran PJ. 1999. Estimating canopy chlorophyll concentration from field and airborne spectra. *Remote Sensing of Environment* **68,** 217–224.

Kebabian PL, Theisen AF, Kallelis S, Freedman A. 1999. A passive two-band sensor of sunlight-excited plant fluorescence. *Review of Scientific Instruments* **70,** 4386–4393.

Knyazikhin Y, Martonchik JV, Myneni RB, Diner DJ, Running SW. 1998. Synergistic algorithm for estimating vegetation canopy leaf area index and fraction of absorbed photosynthetically active radiation from MODIS and MISR data. *Journal of Geophysical Research–Atmospheres* **103,** 32257–32275.

Kolber Z, Klimov D, Ananyev G, Rascher U, Berry J, Osmond B. 2005. Measuring photosynthetic parameters at a distance: laser induced fluorescence transient (LIFT) method for remote measurements of photosynthesis in terrestrial vegetation. *Photosynthesis Research* **84,** 121–129.

Krause GH, Weis E. 1991. Chlorophyll fluorescence and photosynthesis: the basics. *Annual Review of Plant Physiology and Plant Molecular Biology* **42,** 313–349.

Lichtenthaler HK, Rinderle U. 1988. The role of chlorophyll fluorescence in the detection of stress conditions in plants. *Critical Reviews in Analytical Chemistry* **19,** S29–S85.

Lichtenthaler HK, Schweiger J. 1998. Cell wall bound ferulic acid, the major substance of the blue-green fluorescence emission of plants. *Journal of Plant Physiology* **152,** 272–282.

Liesenberg V, Galvao LS, Ponzoni FJ. 2007. Variations in reflectance with seasonality and viewing geometry: implications for classification of Brazilian savanna physiognomies with MISR/Terra data. *Remote Sensing of Environment* **107,** 276–286.

Liu J, Chen JM, Cihlar J, Park WM. 1997. A process-based boreal ecosystem productivity simulator using remote sensing inputs. *Remote Sensing of Environment* **62,** 158–175.

Liu LY, Zhang YJ, Wang JH, Zhao CJ. 2005. Detecting solar-induced chlorophyll fluorescence from field radiance spectra based on the Fraunhofer line principle. *IEEE Transactions on Geoscience and Remote Sensing* **43,** 827–832.

Lopez G, Rubio MA, Martinez M, Batlles FJ. 2001. Estimation of hourly global photosynthetically active radiation using artificial neural network models. *Agricultural and Forest Meteorology* **107,** 279–291.

Lotsch A, Tian Y, Friedl MA, Myneni RB. 2003. Land cover mapping in support of LAI and FPAR retrievals from EOS-MODIS and MISR: classification methods and sensitivities to errors. *International Journal of Remote Sensing* **24,** 1997–2016.

Louis J, Ounis A, Ducruet JM, *et al*. 2005. Remote sensing of sunlight-induced chlorophyll fluorescence and reflectance of Scots pine in the boreal forest during spring recovery. *Remote Sensing of Environment* **96,** 37–48.

Lucas NS, Curran PJ. 1999. Forest ecosystem simulation modelling: the role of remote sensing. *Progress in Physical Geography* **23,** 391–423.

Lucas RM, Honzak M, Curran PJ, Foody GM, Milne R, Brown T, Amaral S. 2000. Mapping the regional extent of tropical forest regeneration stages in the Brazilian Legal Amazon using NOAA AVHRR data. *International Journal of Remote Sensing* **21,** 2855–2881.

Malenovský Z, Albrechtová J, Lhotáková Z, Zurita-Milla R, Clevers J, Schaepman ME, Cudlín P. 2006. Applicability of the PROSPECT model for Norway spruce needles. *International Journal of Remote Sensing* **27,** 5315–5340.

Martel MC, Margolis HA, Coursolle C, Bigras FJ, Heinsch FA, Running SW. 2005. Decreasing photosynthesis at different spatial scales during the late growing season on a boreal cutover. *Tree Physiology* **25,** 689–699.

Martin ME, Newman SD, Aber JD, Congalton RG. 1998. Determining forest species composition using high spectral resolution remote sensing data. *Remote Sensing of Environment* **65,** 249–254.

McDonald AJ, Gemmell FM, Lewis PE. 1998. Investigation of the utility of spectral vegetation indices for determining information on coniferous forests. *Remote Sensing of Environment* **66,** 250–272.

McFarlane JC, Watson RD, Theisen AF, Jackson RD, Ehrler WL, Pinter PJ, Idso SB, Reginato RJ. 1980. Plant stress detection by remote measurement of fluorescence. *Applied Optics* **19,** 3287–3289.

McVicar TR, Jupp DLB. 1998. The current and potential operational uses of remote sensing to aid decisions on drought exceptional circumstances in Australia: a review. *Agricultural Systems* **57,** 399–468.

Measures RM, Houston W, Bristow M. 1973. Development and field-tests of a laser fluorosensor for environmental monitoring. *Canadian Aeronautics and Space Journal* **19,** 501–506.

Meroni M, Colombo R. 2006. Leaf level detection of solar induced chlorophyll fluorescence by means of a subnanometer resolution spectroradiometer. *Remote Sensing of Environment* **103,** 438–448.

Methy M. 2000. Analysis of photosynthetic activity at the leaf and canopy levels from reflectance measurements: a case study. *Photosynthetica* **38,** 505–512.

Meyer S, Cartelat A, Moya I, Cerovic ZG. 2003. UV-induced blue-green and far-red fluorescence along wheat leaves: a potential signature of leaf ageing. *Journal of Experimental Botany* **54,** 757–769.

Mishra KB, Gopal R. 2008. Detection of nickel-induced stress using laser-induced fluorescence signatures from leaves of wheat seedlings. *International Journal of Remote Sensing* **29,** 157–183.

Morales F, Cerovic ZG, Moya I. 1996. Time-resolved blue-green fluorescence of sugar beet (*Beta vulgaris* L) leaves. Spectroscopic evidence for the presence of ferulic acid as the main fluorophore of the epidermis. *Biochimica et Biophysica Acta* **1273,** 251–262.

Moya I, Camenen L, Evain S, Goulas Y, Cerovic ZG, Latouche G, Flexas J, Ounis A. 2004. A new instrument for passive remote sensing. 1. Measurements of sunlight-induced chlorophyll fluorescence. *Remote Sensing of Environment* **91,** 186–197.

Moya I, Cerovic ZG. 2004. Remote sensing of chlorophyll fluorescence: instrumentation and analysis. In: Papageorgiou GC, Govindjee, eds. *Chlorophyll* a *fluorescence: a signature of photosynthesis*. Dordrecht: Springer, 429–445.

Moya I, José M, Laurila T, Stoll M-P, Miller J. 2003. Photosynthesis from space: a new vegetation fluorescence technique. *ESA Bulletin* **116,** 34–37.

Myneni RB, Hoffman S, Knyazikhin Y, *et al*. 2002. Global products of vegetation leaf area and fraction absorbed PAR from year one of MODIS data. *Remote Sensing of Environment* **83,** 214–231.

Myneni RB, Maggion S, Iaquinta J, Privette JL, Gobron N, Pinty B, Kimes DS, Verstraete MM, Williams DL. 1995. Optical remote sensing of vegetation: modeling, cavaets, and algorithms. *Remote Sensing of Environment* **51,** 169–188.

Myneni RB, Williams DL. 1994. On the relationship between *FAPAR* and NDVI. *Remote Sensing of Environment* **49,** 200–211.

Nedbal L, Koblížek M. 2006. Chlorophyll fluorescence as a reporter on *in vivo* electron transport and regulation in plants. In: Grimm B, Porra R, Rüdiger W, Scheer H, eds. *Biochemistry and biophysics of chlorophylls*. Dordrecht, The Netherlands: Springer, 507–519.

Nedbal L, Soukupová J, Kaftan D, Whitmarsh J, Trtílek M. 2000. Kinetic imaging of chlorophyll fluorescence using modulated light. *Photosynthesis Research* **66,** 3–12.

Niyogi KK. 1999. Photoprotection revisited: genetic and molecular approaches. *Annual Review of Plant Physiology and Plant Molecular Biology* **50,** 333–359.

Nolin AW. 2004. Towards retrieval of forest cover density over snow from the Multi-angle Imaging SpectroRadiometer (MISR). *Hydrological Processes* **18,** 3623–3636.

Olioso A, Méthy M, Lacaze B. 1992. Simulation of canopy fluorescence as a function of canopy structure and leaf fluorescence. *Remote Sensing of Environment* **41,** 239–247.

Omasa K, Shimazaki KI, Aiga I, Larcher W, Onoe M. 1987. Image-analysis of chlorophyll fluorescence transients for diagnosing the photosynthetic system of attached leaves. *Plant Physiology* **84,** 748–752.

Ounis A, Cerovic ZG, Briantais JM, Moya I. 2001. Dual-excitation FLIDAR for the estimation of epidermal UV absorption in leaves and canopies. *Remote Sensing of Environment* **76,** 33–48.

Pedrós R, Goulas Y, Jacquemoud S, Louis J, Moya I. 2005. A new leaf fluorescence model. *2nd International workshop on remote sensing of vegetation fluorescence*. 17–19 November 2004, Canadian Space Agency Conference Center, St-Hubert, Québec, Canada.

Pedrós R, Moya I, Goulas Y, Jacquemoud S. 2008. Chlorophyll fluorescence emission spectrum inside a leaf. *Photochemical and Photobiological Science* **7,** 498–502.

Pfündel E. 1998. Estimating the contribution of Photosystem I to total leaf chlorophyll fluorescence. *Photosynthesis Research* **56,** 185–195.

Plascyk JA. 1975. Mkli Fraunhofer line discriminator (FLD-li) for airborne and orbital remote-sensing of solar-stimulated luminescence. *Optical Engineering* **14,** 339–346.

Plascyk JA, Gabriel FC. 1975. Fraunhofer line discriminator Mkli: airborne instrument for precise and standardized ecological luminescence measurement. *IEEE Transactions on Instrumentation and Measurement* **24,** 306–313.

Potter CS, Randerson JT, Field CB, Matson PA, Vitousek PM, Mooney HA, Klooster SA. 1993. Terrestrial ecosystem production: a process model-based on global satellite and surface data. *Global Biogeochemical Cycles* **7,** 811–841.

Price JC. 2003. Comparing MODIS and ETM+ data for regional and global land classification. *Remote Sensing of Environment* **86,** 491–499.

Qi J, Huete AR, Moran MS, Chehbouni A, Jackson RD. 1993. Interpretation of vegetation indexes derived from multitemporal SPOT images. *Remote Sensing of Environment* **44,** 89–101.

Qi J, Kerr YH, Moran MS, Weltz M, Huete AR, Sorooshian S, Bryant R. 2000. Leaf area index estimates using remotely sensed data and BRDF models in a semiarid region. *Remote Sensing of Environment* **73,** 18–30.

Raimondi V, Palombi L, Lognoli D, Cecchi G, Masotti L. 2007. Design and development of a new high speed performance fluorescence imaging lidar for the diagnostics of indoor and outdoor cultural heritage. In: *Proceedings of LACONA VII*: 7th International Conference on Lasers in the Conservation of Artworks, Madrid 17–21 September 2007, Taylor and Francis.

Rascher U, Gioli B, Miglietty F. 2008. FLEX: FLuorescence EXplorer: a remote sensing approach to quantify spatio-temporal variations of photosynthetic efficiency from space. In: Allen JF, Osmond B, Golbeck JH, Gantt E, eds. *Energy from the sun*. Proceedings of the 14th International Congress on Photosynthesis Research 2007. Dordrecht: Springer.

Rascher U, Nedbal L. 2006. Dynamics of plant photosynthesis under fluctuating natural conditions. *Current Opinion in Plant Biology* **9,** 671–678.

Rascher U, Liebig M, Lüttge U. 2000. Evaluation of instant light-response curves of chlorophyll-fluorescence parameters obtained with a portable chlorophyll fluorometer on site in the field. *Plant*, *Cell and Environment* **23,** 1397–1405.

Rasmussen MS. 1998. Developing simple, operational, consistent NDVI-vegetation models by applying environmental and climatic information. Part I. Assessment of net primary production. *International Journal of Remote Sensing* **19,** 97–117.

Rautiainen M, Lang M, Mõttus M, Kuusk A, Nilson T, Kuusk J, Lükk T. 2008. Multi-angular reflectance properties of a hemiboreal forest: an analysis using CHRIS PROBA data. *Remote Sensing of Environment* **112,** 2627–2642.

Richards JT, Schuerger AC, Capelle G, Guikema JA. 2003. Laser-induced fluorescence spectroscopy of dark- and light-adapted bean (*Phaseolus vulgaris* L.) and wheat (*Triticum aestivum* L.) plants grown under three irradiance levels and subjected to fluctuating lighting conditions. *Remote Sensing of Environment* **84,** 323–341.

Richardson AD, Duigan SP, Berlyn GP. 2002. An evaluation of non-invasive methods to estimate foliar chlorophyll content. *New Phytologist* **153,** 185–194.

Rosema A, Verhoef W, Schroote J, Snel JFH. 1991. Simulating fluorescence light-canopy interaction in support of laser-induced fluorescence measurements. *Remote Sensing of Environment* **37,** 117–130.

Rouse JWJ, Haas RH, Schell JA, och Deering DW. 1974. Monitoring vegetation systems in the Great Plains with ERTS. In: Freden SC, Marcanti EP, Becker MA, eds. *NASA SP-351*. Proceedings of the 3rd Earth Resources Technology Satellite-1 Symposium, 1973, NASA Scientific and Technical Information Office, Washington DC. 309–317.

Ruimy A, Dedieu G, Saugier B. 1996. TURC: a diagnostic model of continental gross primary productivity and net primary productivity. *Global Biogeochemical Cycles* **10,** 269–285.

Ruimy A, Kergoat L, Bondeau A. 1999. Comparing global models of terrestrial net primary productivity (NPP): analysis of differences in light absorption and light-use efficiency. *Global Change Biology* **5,** 56–64.

Rundel RD. 1983. Action spectra and estimation of biologically effective UV radiation. *Physiologia Plantarum* **58,** 360–366.

Running SW, Baldocchi DD, Turner DP, Gower ST, Bakwin PS, Hibbard KA. 1999. A global terrestrial monitoring network integrating tower fluxes, flask sampling, ecosystem modeling and EOS satellite data. *Remote Sensing of Environment* **70,** 108–127.

Running SW, Nemani RR, Heinsch FA, Zhao MS, Reeves M, Hashimoto H. 2004. A continuous satellite-derived measure of global terrestrial primary production. *Bioscience* **54,** 547–560.

Saito Y, Matsubara T, Koga T, Kobayashi F, Kawahara TD, Nomura A. 2005. Laser-induced fluorescence imaging of plants using a liquid crystal tunable filter and charge coupled device imaging camera. *Review of Scientific Instruments* **76,** 106–103.

Schreiber U, Schliwa U, Bilger W. 1986. Continuous recording of photochemical and nonphotochemical chlorophyll fluorescence quenching with a new type of modulation fluorometer. *Photosynthesis Research* **10,** 51–62.

Sellers PJ, Tucker CJ, Collatz GJ, Los SO, Justice CO, Dazlich DA, Randall DA. 1994. A global 1-degrees-by-1-degrees NDVI data set for climate studies. 2. The generation of global fields of terrestrial biophysical parameters from the NDVI. *International Journal of Remote Sensing* **15,** 3519–3545.

Sims DA, Gamon JA. 2002. Relationships between leaf pigment content and spectral reflectance across a wide range of species, leaf structures and developmental stages. *Remote Sensing of Environment* **81,** 337–354.

Sioris CE, Courreges-Lacoste GB, Stoll MP. 2003. Filling in of Fraunhofer lines by plant fluorescence: simulations for a nadir-viewing satellite-borne instrument. *Journal of Geophysical Research-Atmospheres* 108, Article number 4133.

Sioris CE, Evans WFJ. 2000. Impact of rotational Raman scattering in the O-2 A band. *Geophysical Research Letters* **27,** 4085–4088.

Soukupová J, Csefalvay L, Urban O, Košvancová M, Marek M, Rascher U, Nedbal L. 2008. Annual variation of the steady-state chlorophyll fluorescence emission of evergreen plants in temperate zone. *Functional Plant Biology* **35,** 63–76.

Stober F, Lang M, Lichtenthaler HK. 1994. Blue-green, and red fluorescence emission signatures of green etiolated and white leaves. *Remote Sensing of Environment* **47,** 65–71.

Stober F, Lichtenthaler HK. 1992. Changes of the laser-induced blue, green and red fluorescence signatures during greening of etiolated leaves of wheat. *Journal of Plant Physiology* **140,** 673–680.

Tucker CJ. 1979. Red and photographic infrared linear combinations for monitoring vegetation. *Remote Sensing of Environment* **8,** 127–150.

Turner DP, Ritts WD, Cohen WB, *et al*. 2006. Evaluation of MODIS NPP and GPP products across multiple biomes. *Remote Sensing of Environment* **102,** 282–292.

van der Tol C, Verhoef W, Rosema A. 2009. A model for chlorophyll fluorescence and photosynthesis at leaf scale. *Agricultural and Forest Meteorology* **149,** 96–105.

van Leeuwen WJD, Huete AR, Laing TW. 1999. MODIS vegetation index compositing approach: A prototype with AVHRR data. *Remote Sensing of Environment* **69,** 264–280.

Verhoef W. 1984. Light-scattering by leaf layers with application to canopy reflectance modeling: the SAIL model. *Remote Sensing of Environment* **16,** 125–141.

Verhoef W. 1985. Earth observation modeling based on layer scattering matrices. *Remote Sensing of Environment* **17,** 165–178.

Verhoef W. 2004. Extension of SAIL to model solar-induced canopy fluorescence spectra. *Proceedings of 2nd International Workshop on Remote Sensing of Vegetation Fluorescence, Saint-Hubert, Canada, 17–19 November, 2004*. European Space Agency.

Veroustraete F, Sabbe H, Eerens H. 2002. Estimation of carbon mass fluxes over Europe using the C-Fix model and Euroflux data. *Remote Sensing of Environment* **83,** 376–399.

Verrelst J, Schaepman ME, Koetz B, Kneubühler M. 2008. Angular sensitivity analysis of vegetation indices derived from CHRIS/PROBA data. *Remote Sensing of Environment* **112,** 2341–2353.

Walter-Shea EA, Norman JM, Blad BL, Robinson BF. 1991. Leaf reflectance and transmittance in soybean and corn. *Agronomy Journal* **83,** 631–636.

Wang Q, Adiku A, Tenhunen J, Granier A. 2005. On the relationship of NDVI with leaf area index in a deciduous forest site. *Remote Sensing of Environment* **94,** 244–255.

Watson RD, Hemphill WR, Hessin TD. 1973. Quantification of the luminescence intensity of natural materials. In: *Management and utilization of remote sensing data. Proceedings of the Symposium*. Sioux Falls, South Dakota, 29 October – 1 November 1973. American Society of Photogrammetry, 364–376.

Weiss M, Baret F. 1999. Evaluation of canopy biophysical variable retrieval performances from the accumulation of large swath satellite data. *Remote Sensing of Environment* **70,** 293–306.

Weiss M, Baret F, Garrigues S, Lacaze R. 2007. LAI and *fAPAR* CYCLOPES global products derived from VEGETATION. Part 2: validation and comparison with MODIS collection 4 products. *Remote Sensing of Environment* **110,** 317–331.

Weiss M, Baret F, Myneni RB, Pragnere A, Knyazikhin Y. 2000. Investigation of a model inversion technique to estimate canopy biophysical variables from spectral and directional reflectance data. *Agronomie* **20,** 3–22.

Xiao X, Boles S, Liu J, Zhuang D, Frolking S, Li C, Salas W, Moore III B. 2005. Mapping paddy rice agriculture in southern China using multi-temporal MODIS images. *Remote Sensing of Environment* **95,** 480–492.

Xiao X, Boles S, Liu J, Zhuang D, Liu M. 2002. Characterization of forest types in Northeastern China, using multi-temporal SPOT-4 VEGETATION sensor data. *Remote Sensing of Environment* **82,** 335–348.

Yoder BJ, Pettigrewcrosby RE. 1995. Predicting nitrogen and chlorophyll content and concentrations from reflectance spectra (400–2500 nm) at leaf and canopy scales. *Remote Sensing of Environment* **53,** 199–211.

Zarco-Tejada PJ, Miller JR, Noland TL, Mohammed GH, Sampson PH. 2001. Scaling-up and model inversion methods with narrowband optical indices for chlorophyll content estimation in closed forest canopies with hyperspectral data. *IEEE Transactions on Geoscience and Remote Sensing* **39,** 1491–1507.

Zarco-Tejada PJ, Miller JR, Pedros R, Verhoef W, Berger M. 2006. FluorMODgui V3.0: A graphic user interface for the spectral simulation of leaf and canopy chlorophyll fluorescence. *Computers and Geosciences* **85,** 577–591.

Zarco-Tejada PJ, Rueda CA, Ustin SL. 2003. Water content estimation in vegetation with MODIS reflectance data and model inversion methods. *Remote Sensing of Environment* **85,** 109–124.

Zhang XY, Friedl MA, Schaaf CB, Strahler AH, Hodges JCF, Gao F, Reed BC, Huete A. 2003. Monitoring vegetation phenology using MODIS. *Remote Sensing of Environment* **84,** 471–475.

Zhang Y, Tian Y, Myneni RB, Knyazikhin Y, Woodcock CE. 2002. Assessing the information content of multiangle satellite data for mapping biomes I. Statistical analysis. *Remote Sensing of Environment* **80,** 418–434.